Clays and Clay Minerals, Vol. 59, No. 5, 538–545, 2011.

STUDY OF THE INTERACTION BETWEEN BENTONITE AND A STRAIN OF *BACILLUS MUCILAGINOSUS*

YUN ZHU[1,2], YAN LI[1], ANHUAI LU[1,*], HAORAN WANG[1], XIAOXUE YANG[1], CHANGQIU WANG[1], WEIZHENG CAO[3], QINGHUA WANG[3], XIAOLEI ZHANG[3], DANMEI PAN[4], AND XIAOHONG PAN[4]

[1] The Key Laboratory of Orogenic Belts and Crustal Evolution, School of Earth and Space Sciences, Peking University, Beijing 100871, China

[2] National Research Center for Geoanalysis, Beijing 100037, China

[3] PetroChina Daqing Oilfield Company Ltd., Exploration and Development Research Institute, Daqing 163712, China

[4] State Key Lab of Structural Chemistry Fujian Institute of Research on the Structure of Matter, Chinese Academy of Sciences Fuzhou, Fujian, 350002, China

Abstract—Mineral-microbe interactions are widespread in a number of environmental processes such as mineral weathering, decomposition, and transformation. Both clay minerals and silicate-weathering bacteria are widely distributed in nature, and the latter contribute to weathering, diagenesis, and mineralization of major rock-forming minerals. The purpose of this study was to observe changes in the chemical composition and structure, especially the phase transformation, of smectite after processing by a silicate-weathering bacterium. The interaction between *Bacillus mucilaginosus* and bentonite was studied using custom culture media. Results from Inductively Coupled Plasma-Atomic Emission Spectrometry revealed that the bacterium promoted release of Si and Al from solid bentonite to solution. Concomitantly, the K and Fe contents of the mineral increased as shown by X-ray photoelectron spectroscopy results. After interaction with the bacterium, the montmorillonite underwent a possible structure transformation to smectite, as indicated by the emergence of a new weak peak (d = 9.08 Å) shown by X-ray diffraction patterns. The mineralogical changes were also demonstrated by the decrease in the specific surface area of the mineral from 33.0 to 24.0 m^2/g (these lower values for SSA of bentonite are related to the particle size of the smectite examined (120−160 mesh) and the weakened absorption bands in Al−O−H and Si−O−Si vibrations by Micro Fourier-transform infrared spectroscopy. The morphology changes in the bacteria observed by environmental scanning electron microscopy and atomic force microscopy revealed an obvious growth of the flagella in the presence of bentonite.

Key Words—*Bacillus mucilaginosus*, Bentonite, Clay Minerals, Microbe-mineral Interaction, Silicate Bacteria, Smectite.

INTRODUCTION

The interactions between microbes and minerals have attracted much attention for the past decade and more (Fortin *et al*., 1998; Ehrlich, 1998; Dong *et al.*, 2009; Dong, 2010). Microbes isolated from either natural smectite or soil extract can reduce the structural Fe(III) in ferruginous smectite (Stucki *et al*., 1987) and nontronite (Wu *et al*., 1988). The physical and chemical properties of smectite, such as clay-particle flocculation, dispersion, swelling, surface area, and cation and anion exchange capacity have been found to be changed significantly by *Shewanella* (Gates *et al*., 1993; Kostka *et al*., 1999; Stucki *et al.*, 2002; Stucki and Kostka, 2006; Kim *et al.*, 2005; Jaisi, 2007). Kim *et al*. (2004) concluded that microbial reduction of Fe(III) in Fe-rich smectite could promote the transformation from smectite to illite. Most of these studies have focused on mineral transformations promoted by dissimilatory metal-reducing bacteria. Others have studied the dissolution of minerals induced by microbial metabolism, representing an alternative interactive pathway between minerals and microbes. Maurice *et al.* (2001) studied enhancement of kaolinite dissolution by aerobic *Pseudomonas mendocina*, and, as a result of dissolution, a trace amount of Fe was released from the mineral to support microbial growth; *Piloderma* was found (Glowa *et al.*, 2003) to extract nutrients (Mg and K) from biotite, microcline, and chlorite in soils. In these processes, the microbe-mineral interactions were not accompanied by valence change of the metal ions. Whether such an interactive mechanism could cause structural transformation of minerals remains unknown.

Silicate-weathering bacteria such as *Bacillus mucilaginosus*, *Bacillus circulans*, and *Bacillus edaphius* are widely distributed in nature and contribute to weathering, diagenesis, and mineralization of major rock-forming minerals such as silicates. The so-called 'silicate bacterium' is generally accepted to refer to *Bacillus mucilaginosus*, which was first discovered and isolated from silicate minerals in 1939 (Aleksandrov, 1953). Previous studies have shown that *Bacillus*

* E-mail address of corresponding author:
ahlu@pku.edu.cn
DOI: 10.1346/CCMN.2011.0590511

mucilaginosus can dissolve K in K-rich silicate minerals such as mica and illite and can extract P from apatite; hence, the bacterium has been used as a biological fertilizer to accommodate plant growth in barren soil (Boyle and Voigt, 1973; Lian, 1998; Liu *et al*., 2006; Li *et al.*, 2007). The ability of this bacterium to decompose minerals makes it a good candidate for the extraction of Si and Al from bauxite in the metallurgical industry (Monib *et al.*, 1986). In addition, the generation of a mass of zoogloea by extracellular polymeric substances during its growth allows *Bacillus mucilaginosus* to be used as a bio-flocculant for wastewater treatment (Lian *et al.*, 2008).

Bentonite, which is composed mainly of the layered silicate smectite and small amounts of other silicate minerals such as quartz and feldspar, has been used widely in environmental and geotechnology-related applications (Emmerich *et al.*, 2009), such as in cat litter and other odor adsorbents, paint, the paper industry, the foundry industry, in wastewater treatment, and in bleaching agents in the food industry (Harvey and Lagaly, 2006). However, the composition and structure of bentonite may be affected by certain microorganisms, which lead to changes in the physical and chemical properties of the bentonite and therefore limit its application under some conditions.

The objective of the present study was to investigate the interaction between bentonite and a common representative silicate bacterium, *Bacillus mucilaginosus*. Observations of crystal-structure changes during the interaction process would provide direct evidence of the role of *Bacillus mucilaginosus* in the dissolution or transformation of layered silicate minerals.

MATERIALS AND METHODS

Bacteria and minerals

The bacterial strain used in the present study was kindly donated by the Soil and Fertilizer Institute, Chinese Academy of Agricultural Sciences, and was identified as *Bacillus mucilaginosus* by 16s rDNA analysis. The bacterial strain was Gram negative and bacilliform (no flagella observed under AFM), and was 1.0−1.2 μm × 2.5−7 μm in size. Previous reports did not define whether it has flagella. Before inoculation, the culture was maintained on agar slants and stored at 4ºC.

The clay-rich rock used for this study was a bentonite sample from Jianping district of Liaoning Province, China. The bentonite deposit is located at the southern edge and in the eastern part of inner Mongolia and is hosted by Archean basement gneiss. The deposit is in andesitic tuff breccia, tuffaceous sandstone, rhyolite, and rhyolitic tuff gravel of the lower part of the Yixian Formation, which is a lacustrine volcano-sedimentary deposit (Yin, 2005). The bentonite consists of 65% smectite, 10% quartz, 10% calcite, 10% feldspar, and ~5% dolomite.

Culture medium and experimental procedures

Two types of culture media were used (The People's Republic of China agricultural standards NY882-2004, 2004): (1) Seed liquid: 5.0 g/L of starch, 1.0 g/L of yeast extract, 0.2 g/L of K_2HPO_4, 0.5 g/L of $MgSO_4{\cdot}7H_2O$, 0.1 g/L of $CaCO_3$, and 5 mg/L of $FeCl_3{\cdot}6H_2O$ (pH 7.5, adjusted with 1 M KOH), for the initial growth (this culture medium can be used for determining easily whether the bacteria were a pure culture); and (2) Growth media: 10.0 g/L of sucrose, 0.5 g/L of $MgSO_4{\cdot}7H_2O$, 0.2 g/L of $(NH_4)_2{\cdot}SO_4$, 0.1 g/L of KCl, 0.1 g/L of $CaCO_3$ (pH 7.5, adjusted with 1 M HCl). The bacteria were covered with a slimy coating, consisting mainly of peptidoglycan and metabolites in the growth media, both of which accelerated the dissolution of the silicate minerals.

A 1.0 g bentonite sample was added to 200 mL of the growth media. The experiments were conducted in 500 mL glass flasks, which were sealed using sealing film for sterile culture vessels. Prior to the experiments, all bottles were autoclaved at 121ºC and 1 atm for 20 min.

Twenty-one flasks, each containing 200 mL of the growth media and 1.0 g of the bentonite, were divided into three groups: one group of seven to be used as a control group, *i.e.* to which no bacteria were added (Blank), and the other two groups of seven bottles to be used as parallel experimental groups to which bacteria were added (BM1 and BM2).

One or two loops of the selected strain were inoculated into 100 mL of seed liquid, and the culture was then incubated at a constant temperature of 30ºC and cultured at an oscillating speed of 150 rpm. After 2 days, 1 mL of the bacterial culture was used to inoculate the bentonite suspensions in the seven bottles from each of the two parallel experiments receiving bacteria. The experimental conditions were the same as those used in the growth experiments.

Over the course of the experiments, one bottle from each group was sacrificed each day. The bentonite-bacteria suspension was centrifuged at room temperature and with a centrifugal force of 12500 × g for 15 min. For micro-morphology and other physical/chemical analysis, the solid minerals were allowed to air dry and then ground into powder in an agate mortar by hand. The sample obtained was between 80 and 100 μm in size. The supernatant was analyzed using an Inductively Coupled Plasma-Atomic Emission Spectrometer (ICP-AES) to determine the concentration of major elements, such as Si and Al.

Measurement techniques

The growth curves of the strains were monitored using a UV-2102PC ultraviolet/visible (UV/Vis) spectrophotometer (Unico Instruments Co., Ltd., Shanghai, China). The acidity of the supernatant after centrifugation was measured using a FastEasy-50 pH meter (Mettler-Toledo, Switzerland). After adding 2 mL of

https://doi.org/10.1346/CCMN.2011.0590511 Published online by Cambridge University Press

30% hydrogen peroxide to 10 mL of supernatant, the supernatant was heated at 60ºC for 1 h to digest any organic matter. Approximately 5 mL of deionized water was added during the heating process, and the final volume was maintained at 10 mL. Aqueous concentrations of Si and Al were determined using an ICP-AES.

The bacteria-mineral associations at the end of the experiments were examined using an FEI Quanta 200FEG environmental scanning electron microscope (ESEM) (FEI Company, Eindhoven, the Netherlands), and a Veeco Multimode NS3A-02NanoscopeIII atomic force microscope (AFM) (Veeco Instruments, Santa Barbara, California, USA). The ESEM was operated at low vacuum mode with an accelerating voltage of 15 kV, and a short working distance of between 9 and 10 nm. The AFM images were obtained in 'tapping' mode. The cantilever of the tip was a standard 115−135 μm long microlever with a force constant of 20−80 N/m and a typical resonant frequency of between 200 and 400 kHz.

After bacterial treatment, the minerals were analyzed by XRD, XPS, Micro-FTIR, and by means of the BET method of analysis of surface area and pore size. The XRD analyses were performed on a 12 kV Rigaku-RA high-power spinning anode X-ray diffraction apparatus (Rigaku, Japan) using CuKα radiation (λ = 1.5406 Å). The samples were scanned from 3 to 70º2θ at a speed of 8º/min and from 2.5 to 30º2θ at a speed of 2º/min. The ICP-AES was performed using a Profile_Spec instrument (Leeman Labs Inc., Lowell, Massachusetts, USA). The XPS data were collected on an AXIS-Ultra instrument from Kratos Analytical (Manchester, UK) using monochromatic AlKα radiation (225 W, 15 mA, 15 kV) and low-energy electron flooding for charge compensation. Micro-FTIR spectroscopy was carried out using a Nicolet iN10 MX Micro-Fourier transform infrared spectrometer (Nicolet, Madison, Wisconsin, USA) at a resolution of 4 cm^{-1} and the samples were measured from 600 to 4000 cm^{-1}. Each sample was scanned twice and an average value chosen. The BET surface area determination was carried out on an ASAP2010 surface area and pore-size analyzer (Micromeritics Co., Norcross, Georgia, USA) using N_2.

RESULTS AND DISCUSSION

Bacterial growth

The growth of *Bacillus mucilaginosus* was characterized by measuring the optical density at 600 nm (Figure 1). As shown, the bacteria underwent a lag (no apparent growth) phase during the first day, and then went into a logarithmic (log) growth period. As the bacterial cells are metabolically active during this log period, the cells were considered to be suitable for use in inoculation. After 2 days, the bacteria entered a stationary (maintenance) period.

Based on the growth curve of *Bacillus mucilaginosus*, the bacterial cells in their log phase were inoculated into the growth media with minerals. Because of bacterial growth, the pH of the reaction solution (BM) decreased rapidly from 7.5 to 4.3 in the first 2 days, and then stabilized at ~4.5. By contrast, the pH of the abiotic control stabilized at ~7.5 (Figure 1). The decrease in pH was probably due to the production of acidic metabolites such as oxalic acid, tartaric acid, citric acid, and malic acid, *etc*., and of some amino acids (Sun *et al.*, 2006) during growth of the bacteria. When the bacteria went into the stationary growth phase, the metabolic rate and the rate of production of acidic products decreased accordingly, thus resulting in the stable pH values.

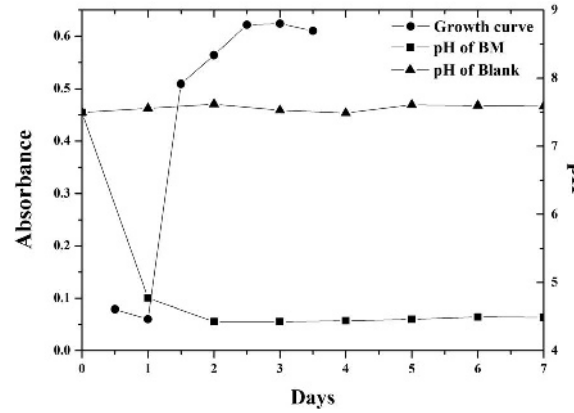

Figure 1. The growth curve of *Bacillus mucilaginosus* and the pH change in the aqueous solution with and without bacterial treatment.

Individual bacteria in association with bentonite were typically rod shaped (Figure 2), consistent with AFM observations (Figure 3). The bacteria in the seed liquid were smooth with no flagella (Figure 3a,b). The bacteria in the growth media without bentonite had no flagella

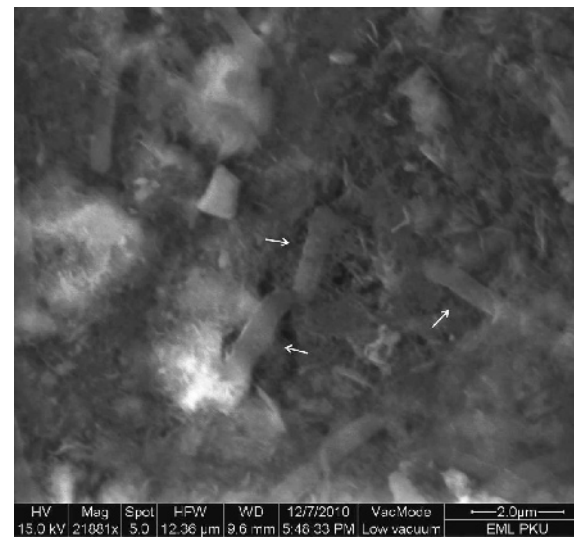

Figure 2. ESEM image showing bacteria (arrows) in association with bentonite.

https://doi.org/10.1346/CCMN.2011.0590511 Published online by Cambridge University Press

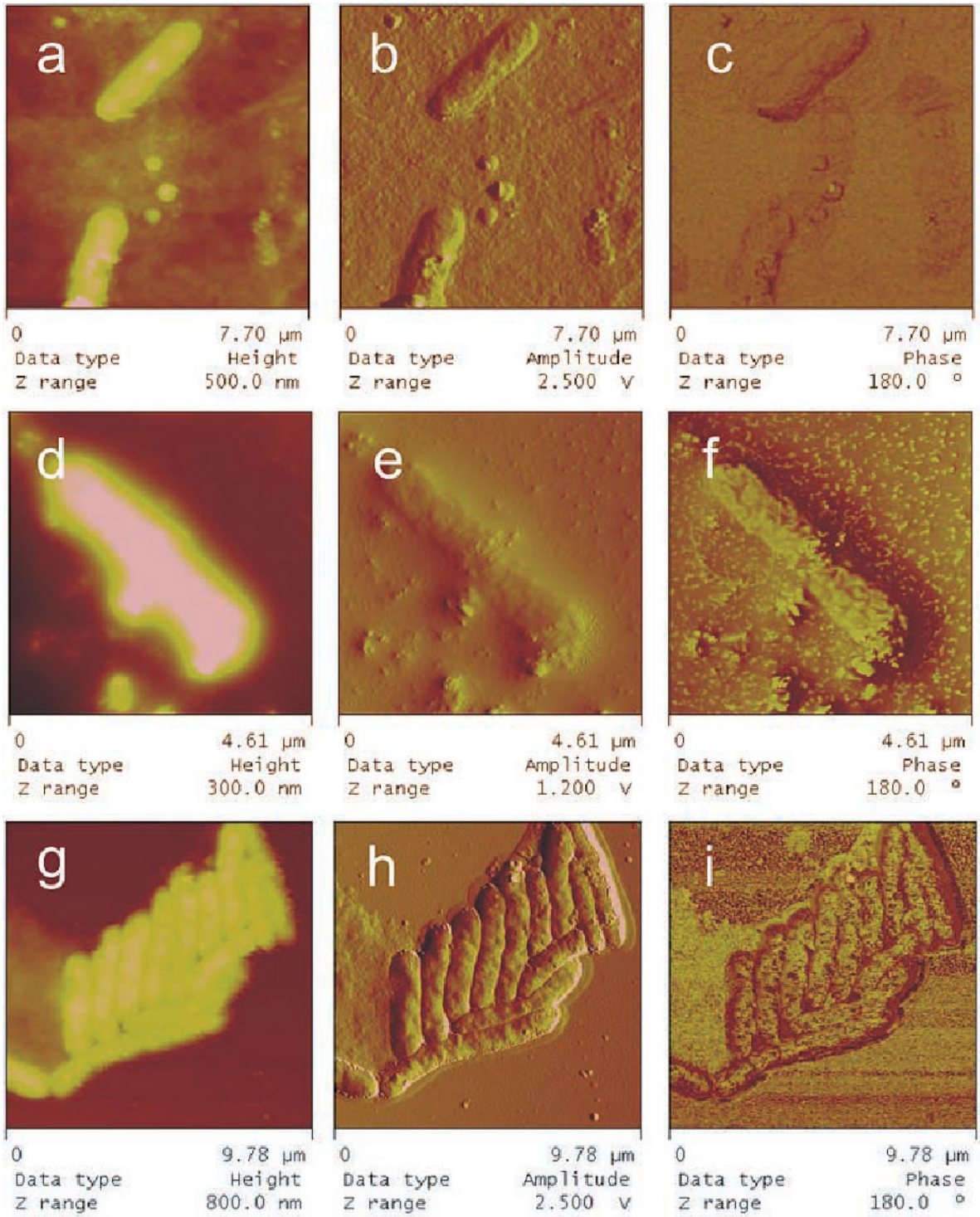

Figure 3. AFM images illustrating the micromorphology of bacteria: typical height, amplitude, and phase images, respectively, of bacteria in different media: (a,b,c) bacteria in seed liquid; (d,e,f) bacteria in growth medium with minerals; and (g,h,i) bacteria in growth medium without minerals.

either (Figure 3 g–i) but flagella were observed in the growth media with bentonite (Figure 3d–f). The emergence of the flagella was clearly related to the presence of bentonite, which could have created a suitable environment for assembly of flagella into flagellar filaments. The bacterial flagellum is thought

https://doi.org/10.1346/CCMN.2011.0590511 Published online by Cambridge University Press

Table 1. Concentration (mg/L) of Si and Al in the culture medium with (BM) and without (Blank) bacteria.

	Si		Al	
Days	Blank	BM	Blank	BM
1	5.47	8.62	0.018	0.49
2	6.77	14.89	0.069	0.493
4	7.03	16.44	0.072	0.795

to facilitate the movement of and attachment of bacteria (Francesco, 1972); sometimes the flagellum is even thought to be involved in the transfer of electrons (Richter *et al.*, 2008). Other effects of the flagellum on mineral dissolution require further study.

Concentration variations of the major dissolved elements

The effect of bacterial growth on mineral decomposition and dissolution was investigated by measuring the concentrations of major elements (Si and Al) released from bentonite into the culture medium. The concentration of both these elements in the BM solution increased with time, suggesting the dissolution of bentonite (Table 1). The Blank solution without bacterial inoculation revealed no changes in the Si and Al concentrations from day 1 to day 4, indicating that the dissolution of the minerals was related to bacterial activity. Based on the data shown in Table 1, the rate of dissolution of Si was calculated to be 6.27 mg/L/day during the log phase, while it decreased to 0.77 mg/L/day during the stationary phase. The rate of release of Si from the mineral structure was consistent with the growth rate of the bacteria, which again demonstrated that the bentonite decomposed as a result of the bacterial activity. In brief, acidic metabolites produced during the bacterial growth might promote the dissolution of the clay minerals.

The concentrations of Si and Al in the solution after bacterial treatment reflected indirectly the chemical compositions of the original mineral. The direct changes of mineral compositions were indicated by XPS results. The atomic ratios of the major elements in bentonite with and without bacterial treatment (Table 2) were compared in proportion to Si, which was the most common element in bentonite (Table 3). After bacterial treatment, a significant increase in the proportion of K in the mineral structure was observed, probably due to the incorporation of K^+ from the culture medium into the interlayer space of the bentonite (smectite). The atomic ratio of K to Si in the smectite structure after bacterial treatment (0.012) was much greater than when no bacteria had been introduced (0.007), which indicated that more K was incorporated under the influence of bacteria. The atomic ratio of Al to Si increased slightly from 0.355 to 0.360, consistent with the ICP-AES results, which showed that the amounts of Si and Al dissolved were different and followed the sequence Si > Al.

In a previous study, Liu *et al.* (2006) found that the bacteria *Bacillius mucilagiosus* failed to dissolve feldspar. Changes in the amounts of Si and Al in solution are, therefore, largely due to dissolution of smectite in the bentonite.

Phase analysis of the clay mineral after bacterial treatment

To further determine whether any changes occurred in the structures of major minerals in the bentonite samples, the BM and Blank samples were characterized by XRD (Figure 4). Both sets of samples showed the same characteristic peaks of smectite, feldspar, and quartz. Calcite disappeared in BM dissolution products, possibly as a result of dissolution of calcite by the acidic metabolic products of the bacteria. A new, weak peak appeared at between 9 and 10º2θ after bacterial treatment. In order to assign the new peak, oriented samples of both the Blank and BM samples were used for XRD over a smaller 2θ range and at a slower speed (Figure 5). The new peak in the BM sample still appeared at 9.77º2θ and was assigned as a characteristic peak of mixed-layer illite-smectite; the same peak was also recorded in previous studies (*e.g.* Zhang *et al.*, 2007) of the illitization of smectite caused by bacterial activity.

Other changes in the clay mineral after bacterial treatment

To prove bacteria-driven structural transformation of the bentonite, Micro-FTIR spectra were collected and BET specific surface area (SSA) measurements taken of the minerals under different treatment conditions. Micro-FTIR spectra of the minerals in both the Blank

Table 2. XPS elemental analyses (relative atomic proportion based on peak areas of the bentonite solid phase before (Blank) and after (BM) bacterial treatment (the results are the averages of three analyses).

Samples	Fe	K	Si	Al	Mg
Blank	1.78	0.12	16.98	6.03	1.62
BM treated	1.74	0.19	15.72	5.66	1.48

Table 3. Atomic ratios of Fe, K, Al, and Mg to Si (the results are the averages of three XPS analyses) before (Blank) and after (BM) treatment with bacteria.

Samples	Fe/Si	K/Si	Al/Si	Mg/Si
Blank	0.10	0.007	0.355	0.095
BM	0.11	0.012	0.360	0.094

https://doi.org/10.1346/CCMN.2011.0590511 Published online by Cambridge University Press

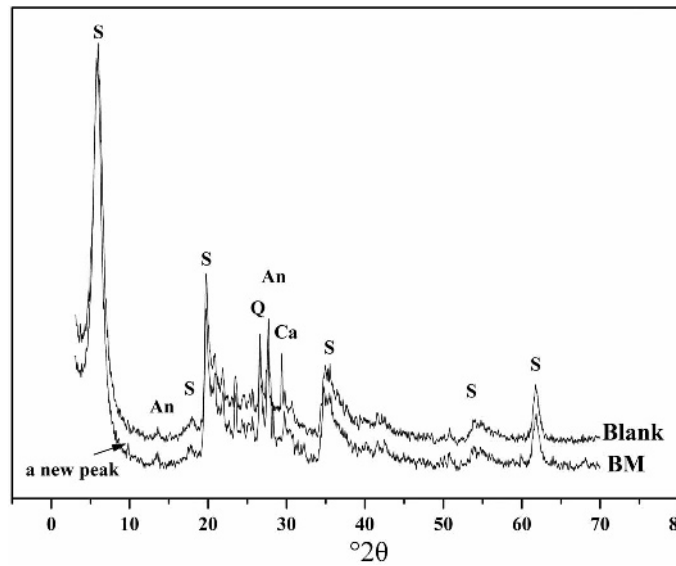

Figure 4. XRD patterns for minerals untreated (Blank) and following bacterial treatment (BM), in random orientation. An: feldspar; Ca: calcite; Q: quartz; S: smectite.

and BM treatments (Figure 6) revealed an absorption peak at ~3620 cm^{-1} assigned to Al−O−H stretching vibrations, and peaks at 3400 cm^{-1} and 1635 cm^{-1} due to the stretching and bending vibrations of H−O−H, respectively. Bacterial treatment of the bentonite (BM) shifted the absorption peaks at 3620 cm^{-1} and 3400 cm^{-1} to higher wavenumbers and the intensities decreased. The intensity of the weak absorption peak at 1635 cm^{-1} also decreased, indicating that the Al-O-H and H-O-H contents in the mineral had decreased. The strongest absorption peak, at 1037 cm^{-1}, was attributed to the antisymmetric stretching vibrations of Si−O−Si, and the weak absorption peak at 795 cm^{-1} was also ascribed to the vibrations of Si−O−Si. After the bacterial treatment, changes in these two absorption peaks were minimal, indicating that the Si−O−Si vibrations still accounted for the strongest and most numerous bonds in the mineral structure. The weak absorption peak which appeared at 918 cm^{-1} was assigned to Al−O−H vibrations, and was reported to be sensitive to changes in Mg and Al content (Farmer, 1982 ; Slosiarikova *et al.*, 1992; Srasra *et al.*, 1994). As the Al content decreased, the intensity of the 918 cm^{-1} peak weakened and its position was slightly lower,

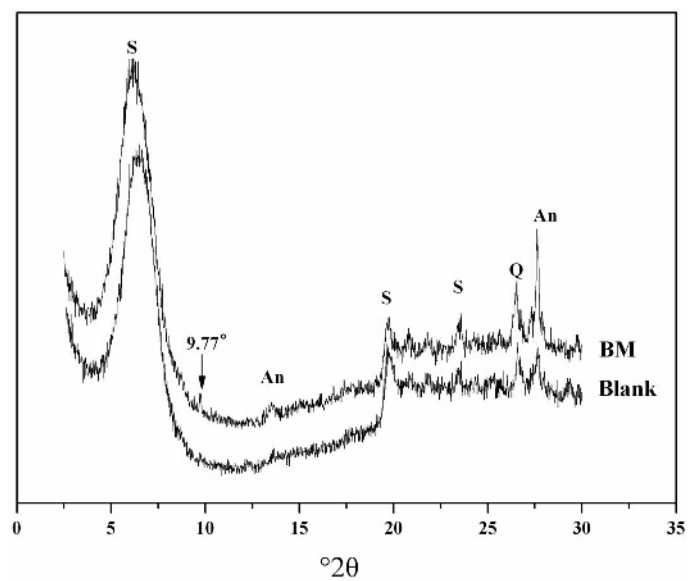

Figure 5. XRD patterns for minerals untreated (Blank) and and following bacterial treatment (BM), oriented. An: feldspar; Q: quartz; S: smectite.

https://doi.org/10.1346/CCMN.2011.0590511 Published online by Cambridge University Press

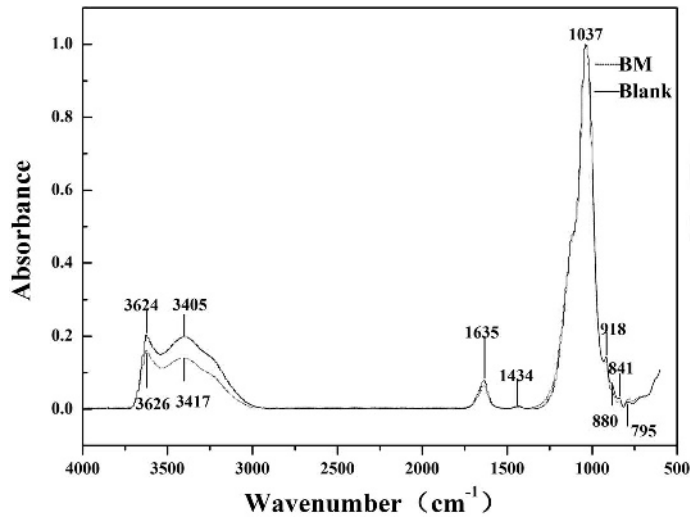

Figure 6. Micro-FTIR absorption spectra of minerals (untreated) and following bacterial treatment (BM).

indicating that the amount of Al in the smectite structure had decreased. The two absorption peaks at 1434 cm^{-1} and 880 cm^{-1} were ascribed to the CO_3^{2-} band, and this was due to the existence of a small proportion of calcite in the bentonite. The disappearance of the CO_3^{2-} bands at 1434 cm^{-1} and 880 cm^{-1} after bacterial treatment was consistent with the XRD results that the calcite disappeared due to the production of acidic metabolites by bacteria.

Mineralogical changes of the minerals in the bentonite sample led to structural and bonding changes resulting in a decrease in the SSA of the bentonite after the bacterial treatment, from 33.0 m^2/g to 24.0 m^2/g (these lower values for SSA of bentonite are related to the particle size of the smectite examined (120–160 mesh)).

Based on pH changes, variations in the major elements in aqueous solution, solid-phase FTIR spectroscopy, and SSA changes, the total process could be described as follows: the production of acidic metabolites during bacterial growth led to dissolution of some of the minerals in the bentonite, probably smectite; continued dissolution caused physical and chemical changes, *e.g.* to the surface area and structure.

CONCLUSIONS

Bacillus mucilaginosus dissolved some of the minerals in bentonite and released Si and Al. With the growth of bacteria, the pH of the culture media decreased. In addition, as a result of bacterial activity, the amounts of K and Fe increased and that of Al decreased in the composition of the remaining solid minerals. The XRD and Micro-FTIR results supported major changes in the minerals in the bentonite. Contact between solid minerals and bacteria appeared to have stimulated the production of bacterial flagella.

The interaction between *Bacillus mucilaginosus* and bentonite proceeded as follows: bacteria produced a certain amount of metabolites and flagella by mineral stimulation. The action of these metabolites and flagella released ions from minerals which led to phase changes in some of the major minerals in the bentonite.

ACKNOWLEDGMENTS

The present study was supported by the National Basic Research Program of China (973 Program, No. 2007 CB815602) and in cooperation with the project in Daqing Oilfield (No. 2009-JS-1006).

REFERENCES

Aleksandrov, V.G. (1953) *Silicate Bacteria*. Science Publishing House, Beijing.

Boyle, J.R. and Voigt, G.K. (1973) Biological weathering of silicate for tree nutrition and soil genesis. *Plant and Soil*, **38**, 191–201.

Dong, H.L. (2010) Mineral-microbe interactions: a review. *Frontiers of Earth Science in China*, **4**, 127–147.

Dong, H.L., Jaisi, D.P., Kim, J., and Zhang, G.X. (2009) Microbe-clay mineral interactions. *American Mineralogist*, **94**, 1505–1519.

Ehrlich, H.L. (1998) Geomicrobiology: its significance for geology. *Earth-Science Reviews*, **45**, 45–60.

Emmerich, K., Wolters, F., Kahr, G., and Lagaly, G. (2009) Clay profiling: the classification of montmorillonites. *Clays and Clay Minerals*, **57**, 101–114.

Farmer, V.C. (1982) *The Infrared Spectra of Minerals* (Chinese version). Science Publishing House, Beijing.

Fortin, D., Ferris, F.G., and Beveridge, T.J. (l998) Surface-mediated mineral development by bacteria. Pp. l61–180 in: *Geomicrobiology: Interactions between Microbes and Minerals* (J.F. Banfield and K.H. Nealson, editors). Reviews in Mineralogy, **35**, Mineralogical Society of America, Washington, D.C.

Francesco, S. (1972) Structure and function of bacterial flagella. *Bolletino di Zoologia*, **39**, 111–118.

Gates, W.P., Wilkinson, H.T., and Stucki, J.W. (1993)

Swelling properties of microbially-reduced ferruginous smectite. *Clays and Clay Minerals*, **41**, 360–364.

Glowa, K.R., Arocena, J.M., and Massicotte, H.B. (2003) Extraction of potassium and/or magnesium from selected soil minerals by *Piloderma*. *Geomicrobiology Journal*, **20**, 99–111.

Harvey, C. and Lagaly, G. (2006) Conventional applications. Pp. 501–540 in: *Handbook of Clay Science* (F. Bergaya, B.K.G. Theng, and G. Lagaly, editors). Elsevier, Amsterdam.

Jaisi, D.P. (2007) Fe(III) reduction in clay minerals and its application to technetium immobilization. 319 pp. PhD dissertation, Miami University, Oxford, Ohio, USA.

Kim, J., Dong, H.L., Seabaugh, J., Newell, S.W., and Eberl, D.D. (2004) Role of microbes in the smectite-to-illite reaction. *Science*, **303**, 830–832.

Kim, J., Furukawa, Y., Dong, H.L., and Newell, S.W. (2005) The effect of microbial Fe(III) reduction on smectite flocculation. *Clays and Clay Minerals*, **53**, 572–579.

Kostka, J.E., Haefele, E., Viehweger, R., and Stucki, J.W. (1999) Respiration and dissolution of Fe(III)-containing clay minerals by bacteria. *Environmental Science & Technology*, **33**, 3127–3133.

Li, X., Wu, Z. Q., Li, W.D., and Yan, R.X. (2007) Growth promoting effect of a transgenic *Bacillus mucilaginosus* on tobacco planting. *Applied Microbial and Cell Physiology*, **74**, 1120–1125.

Lian, B. (1998) A study on how silicate bacteria GY92 dissolves potassium from illite. *Acta Mineralogica Sinica*, **18**, 234–237.

Lian, B., Chen, Y., Zhao, J., Teng, H., Zhu, L.J., and Yuan, S. (2008) Microbial flocculation by Bacillus mucilaginosus: Applications and mechanisms. *Bioresource Technology*, **99**, 4825–4831.

Liu, W.X., Xu, X.S., Yang, X.H., Luo, Y.M., and Christie, P. (2006) Decomposition of silicate minerals by *Bacillus mucilaginosus* in liquid culture. *Environmental Geochemistry and Health*, **18**, 133–144.

Maurice, P.A., Vierkorn, M.A., Hersman, L.E., Fulghum, J.E., and Ferryman, A. (2001) Enhancement of kaolinite dissolution by an aerobic *Pseudomonas mendocina* bacterium. *Geomicrobiology Journal*, **18**, 21–35.

Monib, M., Zahra, M.K., and Abdel-Al, H.A. (1986) Role of silicate bacteria in releasing K and Si from biotite and orthoclase. *Soil Biology and Conservation of the Biosphere*, **2**, 733–743.

Richter, H., McCarthy, K., Nevin, K.P., Johnson, J.P., Rotello, V.M., and Lovley, D.R. (2008) Electricity generation by Geobacter sulfurreducens attached to gold electrodes. *Langmuir*, **24**, 4376–4379.

Slosiarikova, H., Bujdak, J., and Hlavaty, V. (1992) IR spectra of octadecylammonium-montmorillonite in the range of the Si-O vibrations. *Journal of Inclusion Phenomena and Molecular Recognition in Chemistry*, **13**, 267–272.

Srasra, E., Bergaya, F., and Fripiat, J.J. (1994) Infrared spectroscopy study of tetrahedral and octahedral substitutions in an interstratified illite-smectite clay. *Clays and Clay Minerals*, **42**, 237–241.

Stucki, J.W. and Kostka, J.E. (2006) Microbial reduction of iron in smectite. *Comptes Rendus Geoscience*, **338**, 468–475.

Stucki, J.W., Komadel, P., and Wilkinson, H.T. (1987) Microbial reduction of structural iron(III) in smectites. *Soil Science Society of America Journal*, **51**, 1663–1665.

Stucki, J.W., Lee, K., Zhang, L., and Larson, R.A. (2002) The effect of iron oxidation state on the surface and structural properties of smectite. *Pure Applied Chemistry*, **74**, 2079–2092.

Sun, D., Zhang, X., and Zhang, Q. (2006) Leaching effects of metabolites of silicate bacterium on silicate minerals. *Mining and Metallurgical Engineering*, **26**, 27–30.

The People's Republic of China Agricultural Standards, NY882-2004 (2004) Silicate-dissolving bacteria culture.

Wu, J., Roth, C.B., and Low, P.F. (1988) Biological reduction of structural Fe in sodium-nontronite. *Soil Science Society of America Journal*, **52**, 295–296.

Yin, X.P. (2005) The geological and application characteristics of bentonite deposit in Jianping. *China Non-metallic Mining Industry Herald*, **51**, 56–58.

Zhang, G.X., Dong, H.L., Kim, J., and Eberl, D.D. (2007) Microbial reduction of structural Fe^{3+} in nontronite by a thermophilic bacterium and its role in promoting the smectite to illite reaction. *American Mineralogist*, **92**, 1411–1419.

(*Received 30 October 2010; revised 21 November 2011; Ms. 508; A.E. H. Dong*)